Int. J. Electrochem. Sci., 16 **(2021)** 150929, doi: 10.20964/2021.01.64

International Journal of ELECTROCHEMICAL SCIENCE
www.electrochemsci.org

Implementation of Pulsed Current Electro-Fenton Process for Humic Acid Removal from Aqueous Solutions: Optimization and Computational Analysis

Gona Hasani[1], Hiua Daraei[2], Kaan Yetilmezsoy[3,], Gilas Hosseini[2], Fardin Gharibi[2], Afshin Maleki[2,*], Shivaraju Harikaranahalli Puttaiah[4], Fatih Ilhan[3]*

[1] Student Research Committee, Kurdistan University of Medical Sciences, Sanandaj, Iran
[2] Environmental Health Research Center, Research Institute for Health Development, Kurdistan University of Medical Sciences, Sanandaj, Iran
[3] Department of Environmental Engineering, Faculty of Civil Engineering, Yildiz Technical University, 34220, Davutpasa, Esenler, Istanbul, Turkey:
[4] Department of Water and Health, Faculty of Life Sciences, Jagadguru Sri Shivarathreeshwara University, Sri Shivarathreeshwara Nagara, Mysuru-570015, Karnataka, India:
[*]E-mail: yetilmez@yildiz.edu.tr; kyetilmezsoy@gmail.com (K.Y.), maleki43@yahoo.com; malaki@muk.ac.ir (A.M.)

Received: 3 September 2020 / *Accepted:* 16 November 2020 / *Published:* 30 November 2020

The implementation of pulse current in an electro-Fenton process was explored for the removal of humic acid (HA). The impacts of different operating variables, including initial HA concentration (C_0 = 10–50 mg/L), initial pH (pH_0 = 3–10), electrical conductivity (EC_0 = 500–3000 µS/cm), pulse time (T_{pls} = 20–200 min), voltage (V = 5–30 volts), and reaction time (t = 10–60 min) on the removal efficiency of HA were explored. The response surface methodology (RSM) was implemented to decrease the number of experiments, and to evaluate the impacts of the model components and the optimal conditions of the process. The maximum removal efficiency (97.2%) with the lowest electrical energy usage (1.02 kWh/kg HA removal) was obtained with the operating conditions of initial HA concentration 50 mg/L, initial pH 3, electrical conductivity 500 µS/cm, pulse time 20 min, voltage 5 V, and reaction time 60 min. For the best HA removal efficiency, the optimum operating conditions of the model components were determined as initial HA concentration 20 mg/L, initial pH 6, electrical conductivity 526 µS/cm, pulse time 200 min, voltage 5 V, and reaction time 10 min. For HA removal efficiency, the determination coefficient (R^2) of 0.885 and its estimated value of 0.7985 were in line with the adjusted R^2 of 0.8532. This study clarified the considerable effects of such studied process-related parameters as pH, HA concentration, applied voltage, and pulse time, and the findings also revealed that the electro-Fenton process to be a powerful and encouraging application for HA removal.

Keywords: electro-Fenton; electrical energy consumption; experimental design; humic acid removal; pulse current

1. INTRODUCTION

Humic acid (HA) is a natural organic compound that creates crucial problems in potable water treatment systems [1]. Natural organic matters enter water reserves through microbial activity and the decay of plant and animal residuals [2], triggering the regeneration of microorganisms in drinking water distribution systems, and increasing the possibility of microbial contagiousness and heavy metals due to increases in HA level. At the same time, these substances cause color and odor problems in the water [3–5], but more essentially, these matters are known to be responsible for the occurrence of disinfection by-products (DBPs) such as trihalomethanes and haloacetic acids [6,7]. Considering their detrimental impacts, it is necessary to eliminate humic matters from water.

Several techniques including coagulation [8], activated carbon adsorption [9], electrocoagulation [10], membrane filtration [11], biological treatment [12], and ion exchange [13] have been performed to eliminate HA. In recent years, due to the increasing pollution of water resources, the use of effective methods, such as advanced oxidation processes (AOPs), for the water have gained popularity [14]. Among these, the Fenton reagent (mixture of H_2O_2 and Fe^{2+} ion) has drawn considerable interest due to its powerful oxidative properties against organic pollutants [15].

Electro-Fenton (EF) is the most widely used electrochemical advanced oxidation process (EAOP), being based on Fenton's reaction chemistry, for the treatment of acidulous waters [16,17]. In EF, H_2O_2 is continually electro-generated by a carbon-containing cathode (Eq. (1)), and a catalytic amount of Fe^{2+} ion is introduced to the polluted solution to react with it and to yield Fe^{3+} ion and consistent OH^- according to the Fenton's reaction (Eq. (2)) with the optimum pH of around 3.0. The benefits of EF compared to the conventional Fenton's reaction are the in situ formation of H_2O_2 and the cathodic generation of Fe^{2+} ion from the initially added Fe^{3+} via Eq. (3), and thus speeding up the Fenton's reaction (Eq. (2)) and improving the mineralization process [18].

$$O_2 + 2H^+ + 2e^- \rightarrow H_2O_2 \quad (1)$$

$$H_2O_2 + Fe^{2+} \rightarrow Fe^{3+} + .OH + OH^- \quad (2)$$

$$Fe^{3+} + e^- \rightarrow Fe^{2+} \quad (3)$$

The application of electrochemical treatment processes (e.g., electrocoagulation, electro oxidations, and electro-reduction) in the water/wastewater sector has gained attention due to the potential for higher efficiency, fewer secondary pollutants, greater safety, and its ability to be controlled automatically. These techniques can be employed to remove a range of pollutants in water and wastewater, from organic matters to heavy metals. However, even the recent increase in the rate of green electricity production from renewable sources has failed to overcome the energy consumption cost barrier for the practical application of these processes.

In this study, the application of an alternative pulse electric current regime is proposed and assessed as a novel technique to overcome the aforementioned critical drawback associated with electrochemical techniques focusing on the electro-Fenton process. The idea is based on altering electrotic role instead of having a permanent cathode and anode and allowing a resting (quenching) time between the loading of electric potential in each pulse intervals. A reduction in electrode consumption and longer-lasting implemented electrodes as well as reducing energy consumption can be expected through electro-chemistry basics for this proposed regime. As discussed in the result

section, the findings of this study were in line with the expectations, and fully supported the basic idea, while a review of literature revealed the application of an alternative pulse current regime to the electro-Fenton process for the removal of humic organic substances is to be a novel idea.

The primary goals of the present study were to apply a pulse current to the electro-Fenton process for the removal of HA from an aqueous environment and to optimize six important process-related parameters: initial HA concentration (C_0), initial pH (pH_0), electrical conductivity (EC_0), pulse time (T_{pls}), voltage (V), and reaction time (t), to maximize the HA removal efficiency. To identify the optimal conditions in the proposed process and the impacts of the independent variables, a response surface methodology (RSM) [19–21] was employed within the framework of a statistical and mathematical computer analysis.

2. EXPERIMENTAL

2.1. Materials

The HA was sourced from Sigma-Aldrich Co. A stock solution (1 g/L) of HA was prepared by dissolving 1 g of HA in 62.5 mL of NaOH (2 N) solution. After dissolving the HA under alkaline conditions, the volume of the solution was adjusted to 1 L using distilled water with a conductivity of 10 μS/cm at 25°C. This solution was then subjected to magnetic stirring for 48 h and then preserved at 4°C in an absence of light [10]. Prior to the experiment, fresh solutions were prepared at the time of use by diluting the stock solution with distilled water. In this study, KNO_3 was utilized as the background electrolyte, and HCl and NaOH were consumed to adjust the reaction pH. $FeH_8N_2O_8S_2$ (anhydrous) was used to prepare standard ferrous (Fe^{2+}) solutions. All other reagents were bought from Merck Chemical Corp. Aluminum electrodes were obtained from a nearby vendor and cut to a suitable size for the experiment.

2.2. Description of Electro-Fenton (EF) Setup

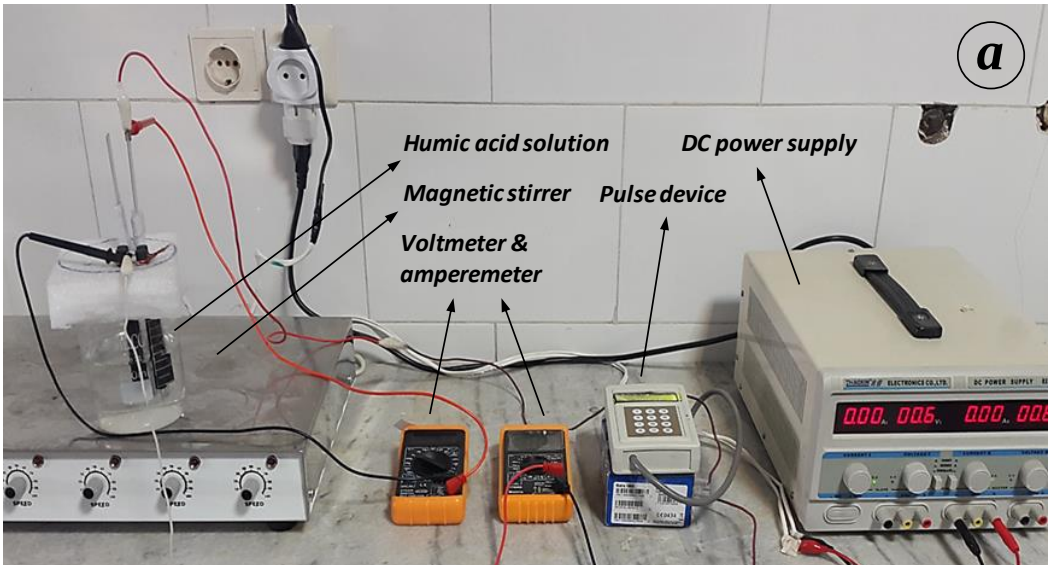

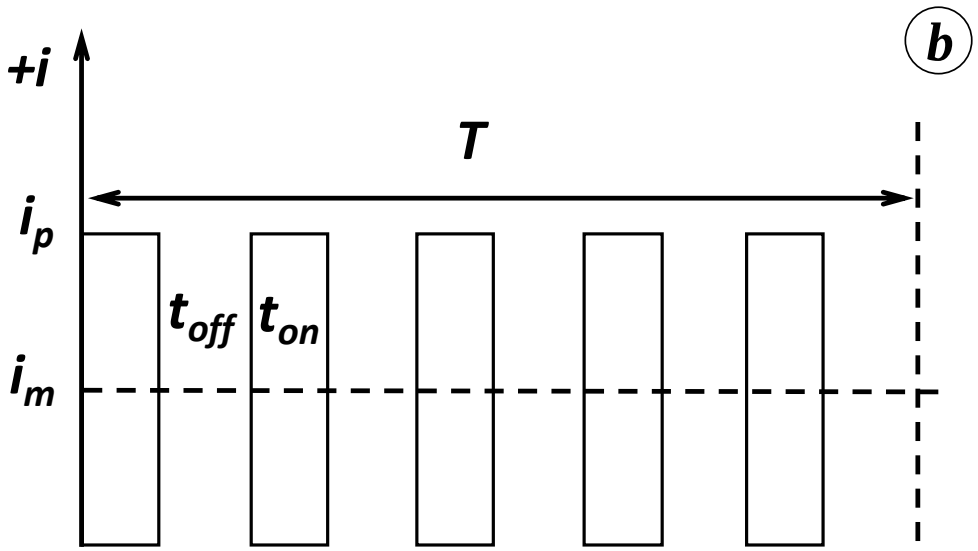

Figure 1. (a) Reactor used for the pulse current electro-Fenton (EF) process; and (b) schematic display of waves of applied pulse current passing through the circuit.

A 600 mL electrochemical cell having two aluminum electrodes as anodes (effective immersed surface area = 30 cm^2) and four-connected graphite electrode as cathode was established. Each cathode electrode comprised of a graphite bar (10 × 120 mm) with a cubic configuration of four electrodes (effective immersed surface area = 3 cm^2). The electrodes were connected to a pulse generator and then to an analog digital DC power supply (RXN-303D-II, Zhaoxin Electronic Tech. Co.) for the experimental measurements. A digitally calibrated pH-meter (Phoenix Ins., EC-30-pH) and a conductivity meter (WTW, Cond 3210) were used to measure the pH value and the electrical conductivity of the solution, respectively. Furthermore, two digital multimeters (Brymen Bm 201), such as an amperemeter and a voltmeter, were utilized to determine the current passing through the circuit and the implemented potential, respectively. A magnetic stirring bar was located on the base of the reactor and rotated at 100 rpm (≈ 10.47 rad/s) throughout the experimentation.

The implemented electro-Fenton reactor with pulse current is depicted in Figure 1a. In the present analysis, the pulse current was applied to save energy usage caused by the time offs between each pulse. Figure 1b illustrates the shape of the pulses formed by the pulser used in this work with a pulse number of 5. As delineated in Figure 1b, after every five square-shaped pulses the electrode positions were altered by altering the direction of the current. In this figure, T refers to the total period, i_p denotes the current density peak, and i_m indicates the average density, t_{on} and t_{off} show the times in case of the current in the circuit is on and off, respectively.

Before the introduction of the HA solution (500 mL) into the EF reactor, the pH was set at chosen initial values (3.0, 6.5, and 10.0) using HCl and NaOH solutions (0.1 N) and also the electrical conductivity was adjusted according to its initial values (500, 1750, and 3000 μS/cm) using KNO_3. The HA concentration was determined via UV absorbance at 254 nm using a UV/Vis spectrophotometer. A standard calibration curve of UV_{254} absorbance versus HA concentrations (0.1–50 mg/L) was developed, and thus the unknown concentration of the sample could be calculated. Overall, HA removal was determined for samples using Eq. (4).

$$HA\ removal\ (mg) = \left(1 - \frac{C}{C_0}\right) \times V \times C_0 \quad (4)$$

where V refers the volume of the solution (L), and C_0 and C indicate the initial and the final HA concentration (mg/L), respectively.

2.3. Design of Experiments

In the present study, the central composite design-response surface methodology (CCD-RSM) was conducted for the optimization of the experimental conditions for HA removal by the EF process. The CCD-RSM is a reliable design system for consecutive experimentation and enables the lack of fit to be tested when a sufficient number of experimental values are provided. In this analysis, a six-factor and a three-level CCD-RSM, with five replications at the center point yielding to a total number of 33 experiments, was performed for response surface modeling. The experiments were carried out in a randomized order.

The independent factors considered in this work were as follows: initial HA concentration (C_0 = 10–50 mg/L), initial pH (pH_0 = 3–10), electrical conductivity (EC_0 = 500–3000 μS/cm), pulse time (T_{pls} = 20–200 min), voltage (V = 5–30 volts), and reaction time (t = 10–60 min). HA removal efficiency (Y) was the dependent factor (or the response variable).

Table 1. Real values of model components and their ranges.

Study Type	RSM			Runs			33				
Initial Design	CCD			Blocks			No Blocks				
Design Model				Quadratic							
Factor	Name	Units	Type	Low actual	High actual	Low coded	High coded	Mean	SD: Standard Deviation		
A	pH	-	Numeric	3	10	-1	+1	6.5	2.585		
B	HA Conc.	mg/L	Numeric	10	50	-1	+1	30	14.771		
C	EC	μS/cm	Numeric	500	3000	-1	+1	1750	923.186		
D	Volt.	V	Numeric	5	30	-1	+1	17.5	9.232		
E	Puls. time	min	Numeric	20	200	-1	+1	110	66.469		
F	Reac. time	min	Numeric	10	60	-1	+1	35	18.464		
Response	Name	Units	Obs.	Analysis	Min.	Max.	Mean	SD	Ratio	Trans.	Model
Y	HA removal	mg	33	Polynomial	0.207	24.30	10.626	6.995	117.391	None	RQuadratic

In the establishment of the CCD matrix, each experiment was employed twice, and repeated five times to ensure replicability. The quadratic (second-order) equation given in Eq. (5) was considered for the CCD-RSM-based analysis of the experimental data [22–24]:

$$Y_{\text{model}} = \beta_0 + \sum_{i=1}^{k} \beta_i x_i + \sum_{i=1}^{k} \beta_{ii} x_i^2 + \sum_{i=1}^{k} \sum_{j=i+1}^{k} \beta_{ij} x_i x_j + \varepsilon \quad (5)$$

where Y is the dependent variable; k is the number of the independent factors; i and j are the index numbers; X_j denote the uncoded independent variables; β_i, β_{ii}, and β_{ij} refer the coefficients of first-order (linear), second-order (quadratic), and interaction terms, respectively; and β_0 demonstrates free or offset term (also called as intercept); and ε connotes is the haphazard error or ambiguities between the estimated and the observed data sets.

In the derivation of Eq. (5), the uncoded independent factors (X_1, X_2, …, X_k) are converted into coded values as follows [22,23]:

$$x_i = \frac{(X_i - X_0)}{\Delta X_i} \quad (6)$$

where x_i is the coded (dimensionless) value of the four process-related variables; X_i is the exact value indicating the four studied variables; X_0 is the actual value of X_i at center point; and ΔX_i denotes the step change in the value. Considering Eq. (6), each of independent factors was coded consecutively as $x_1 = A$: initial pH; $x_2 = B$: initial HA concentration; $x_3 = C$: electrical conductivity; $x_4 = D$: voltage; $x_5 = E$: pulse time; $x_6 = F$: reaction time at three levels: low (-1), center (0), and high (1). The real values of chosen variables and their working limits were selected for the values attained in the preliminary experiments and coded as presented in Table 1. The success of the process was appraised according to the response of HA removal efficiency.

3. RESULTS AND DISCUSSION

3.1. HA Removal Efficiency and Energy Consumption

At run 30, the maximum removal efficiency (97.2%) with the lowest electrical energy usage (1.02 kWh/kg HA removal) was accomplished with the operating conditions of initial HA concentration 50 mg/L, initial pH 3, electrical conductivity 500 μS/cm, pulse time 20 min, voltage 5 V, and reaction time 60 min. On the contrary, at the run 1, the lowest removal efficiency of 4.14% in terms of electrical energy consumption (1871.98 kWh/kg HA or 1.5 kWh/m^3) was attained with the operating conditions of initial HA concentration 10 mg/L, pH_0 10, electrical conductivity 500 μS/cm, pulse time 20 min, voltage 30 V, and reaction time 10 min.

3.2. Derivation of Quadratic Model to Describe HA Removal Efficiency

The experimental HA removal efficiency data were fitted to linear, two-factor interaction (2FI), quadratic, and cubic polynomial structures within the framework of Design Expert software. The models were then compared to check how well they explained the data, and the best-fit equation was chosen. The model terms were reported at a 95% confidence level (p = 0.05) to test their statistical importance in all analyses. Table 2 presents the results of the analysis of variance (ANOVA) for the chosen quadratic model. The model terms with p-values greater than 0.1 were considered unimportant.

A "Lack of Fit (LOF) *F*-value" of 0.51 reveals the LOF to be unnoticeable with respect to the pure error. The *p*-value of 0.8639 for LOF corroborates the unimportance of the model's mistake in portraying the data points within the experimental region.

Table 2. Analysis of variance (ANOVA) for evaluation of the impact of considered factors on the dependent variable and appraising the importance of the proposed model for the EF system.

Response: 1	HA removal					
ANOVA for response surface reduced quadratic model Analysis of variance table (Partial sum of squares – Type III)						
Source	SS	*df*	$MSS = SS/df$ $MSS_E = SS_E/df_E$	$F = \frac{MSS}{MSS_E}$	*p*-value Prob > *F*	Status
Model	1429.62	7	204.23	27.57	< 0.0001	Significant
A – pH	64.97	1	64.97	8.77	0.0066	Significant
B – HA Conc.	1157.57	1	1157.57	156.25	< 0.0001	Significant
D – Volt.	0.43	1	0.43	0.058	0.8113	Not significant
E – Puls. time	40.95	1	40.95	5.53	0.0269	Significant
AD	63.13	1	63.13	9.33	0.0053	Significant
BE	52.05	1	52.05	7.03	0.0137	Significant
E^2	66.82	1	66.82	9.02	0.0060	Significant
Residual	185.21	25	7.41			
Lack of fit	134.67	21	6.41	0.51	0.8639	Not significant
Pure error	50.55	4	12.64			
Cor. Total	1614.84	32				

This statistical measure evaluates the residual error according to the pure error coming from the repeated points in the configured experiments and also clarifies whether or not the model fails to describe the data points, and is thus statistically unimportant [22,25]. In the current ANOVA, the sum of squares due to error, pure error, and LOF are determined from the following equations [22]:

$$SS_E = \sum_{i=1}^{n}\sum_{j=1}^{n_i}(\varepsilon_{ij})^2 = \sum_{i=1}^{n}\sum_{j=1}^{n_i}(Y_{ij} - Y_{pred,i})^2 \quad (7)$$

$$SS_{PE} = \sum_{i=1}^{n}\sum_{j=1}^{n_i}(Y_{ij} - Y_{mean,i})^2 \rightarrow Y_{mean,i} = \frac{1}{n_i}\sum_{i=1}^{n_i} Y_{ij} \quad (8)$$

$$SS_{LOF} = \sum_{i=1}^{n} n_i (Y_{mean,i} - Y_{pred,i})^2 \quad (9)$$

where SS_E refers the total sum of squares due to error ($SS_E = SS_{PE} + SS_{LOF}$); SS_{PE} connotes the sum of squares due to pure error; SS_{LOF} denotes the sum of squares due to LOF; *i* shows an index of each of the *n* different *x* values, *j* is an index of the output variable observed for a given *x* value; n_i is the number of *Y* values related to the i^{th} *x* value; ε_{ij} indicates the difference between the measured and the forecasted responses (residual error); Y_{ij} demonstrates the experimental response of run *i*, replicate *j*; $Y_{pred,i}$ refers the predicted response attained from the proposed polynomial equation for run *i*; and $Y_{mean,i}$ stands for the mean of all replicates for run *i*.

In Table 2, *SS* refers to the sum of squares; *df* indicates the degrees of freedom; *MSS* denotes the mean sum of squares; and *E* is the subscript expressing the error; and *p* values < 0.05 were

regarded as significant. The *F*-value is the test statistic utilized to evaluate whether the term is related to the response; and the *p*-value is a probability that quantifies the proof in comparison with the null hypothesis.

In conclusion, the model's *F*-value of 27.57 reveals that the model is considerable with a very low probability value ($p < F_{\text{model}} = 0.0001$). The probability of such a large "model *F*-Value" occurring due to noise is only 0.01%. The calculated *F* value ($F_{\text{calculated}} = 27.57$) was higher than the tabulated *F* value ($F_{\alpha,df,(n-df+1)} = F_{0.05,7,27} = F_{\text{tabulated}} = 2.37$) at the 5% level [22,23]. This demonstrated that the determined Fisher's variance ratio at this level was sufficiently high to affirm a very elevated degree of fit of the quadratic model and to indicate that the chosen combinations are considerably important [22–24]. Since $F_{\text{calculated}} > F_{\text{tabulated}}$ (27.57 > 2.37), the Fisher's *F*-test at a confidence level of 95% showed that the reduced quadratic polynomial model described a significant amount of the variation in the output component (*Y*: HA removal). The *F*-statistic is obtained in the context of ANOVA as follows [22,23]:

$$F = \frac{\sum_{i=1}^{n} n_i (Y_{mean,i} - Y_{pred,i})^2 \Big/ (n-p)}{\sum_{i=1}^{n}\sum_{j=1}^{n_i} (Y_{ij} - Y_{mean,i})^2 \Big/ (N-n)} = \frac{(SS_{LOF})/d_1}{(SS_{PE})/d_2} \rightarrow N = \sum_{i=1}^{n} n_i \qquad (10)$$

where *p* refers the number of parameters in the model; $d_1 = (n - p)$ and $(N - p)$ indicate the degrees of freedom; *N* denotes the total number of measurements; and the others are described in earlier formula.

3.3. Analysis of Derived Second-order Polynomial Model

Table 3 tabulates the results of the statistical analysis employed on the most appropriate model. The success of fit of the model was further evaluated in terms of the coefficient of determination (R^2). As seen from Table 3, for HA removal efficiency, the R^2 value is 0.885, revealing that only 11.5% of the total variation is not accounted by the model. The R^2 value of 0.885 for the model would ensure a satisfactory correlation between the model-based estimations and the experimental results [22,25]. Additionally, the predicted R^2 (R^2_{pred}) of 0.7985 also shows acceptable agreement with the adjusted R^2 (R^2_{adj}) of 0.8532. Moreover, the signal to noise ratio (S/N) is determined by the adequate precision (AP) and a value larger than 4 is suitable. The AP of 17.356 confirms that the current model reveals an appropriate signal, and can be used to navigate the design space. In the present analysis, the S/N statistic is obtained from Eq. (11) [22]:

$$S/N = \frac{Y_{obs,m} - Y_{pred,m}}{\sigma_{obs} - \sigma_{pred}} = \frac{\left(\frac{1}{n_i}\sum_{i=1}^{n_i} Y_{obs,i}\right) - \left(\frac{1}{n_i}\sum_{i=1}^{n_i} Y_{pred,i}\right)}{\left(\sqrt{\frac{1}{n_i}\sum_{i=1}^{n_i}(Y_{obs,i} - Y_{obs,m})^2}\right) - \left(\sqrt{\frac{1}{n_i}\sum_{i=1}^{n_i}(Y_{pred,i} - Y_{pred,m})^2}\right)} \qquad (11)$$

where $Y_{obs,m}$ refers the mean of observed responses; $Y_{pred,m}$ denotes the mean of the predicted responses; σ_{obs} shows the standard deviation of the observed responses; and σ_{pred} indicates the standard deviation of the predicted responses.

For the current computer-based study, the R^2 and R^2_{adj} values are determined from the following formulas [22,23]:

$$R^2 = 1 - \frac{SS_{res}}{SS_{tot}} = \frac{SS_{tot} - SS_{res}}{SS_{tot}} = \frac{SS_{reg}}{SS_{res} + SS_{reg}} \quad (12)$$

$$R^2 = \frac{\sum_{i=1}^{n}\left(Y_{pred,i} - Y_{obs,mean}\right)^2}{\sum_{i=1}^{n}\left(Y_{obs,i} - Y_{pred,i}\right)^2 + \sum_{i=1}^{n}\left(Y_{pred,i} - Y_{obs,mean}\right)^2} = \frac{\sum_{i=1}^{n}\left(Y_{pred,i} - Y_{obs,mean}\right)^2}{\sum_{i=1}^{n}\left(Y_{obs,i} - Y_{obs,mean}\right)^2} \quad (13)$$

$$R^2_{adj} = 1 - \left(\frac{SS_{res}/df_e}{SS_{tot}/df_t}\right) = 1 - \left[(1-R^2)\left(\frac{n-1}{n-p-1}\right)\right] = R^2 - \left[(1-R^2)\left(\frac{p}{n-p-1}\right)\right] \quad (14)$$

where SS_{tot} denotes the total sum of squares (proportional to the variance of the data); SS_{res} refers the sum of the squares of the residuals (also referred as the residual sum of squares); SS_{reg} indicates the regression sum of squares (also called as the explained sum of squares); p expresses the total number of descriptive variables in the model (except the constant term); n is the size of the sample; df_t explains the degrees of freedom (n – 1) of the forecasted population variance of the response variable; and df_e describes the degrees of freedom (n – p – 1) of the forecast of the population error variance.

"Prob > F" values less than 0.05 reveal the significance of the model terms. For the reduced quadratic model, the results showed that the first-order effects (excepting the voltage) of initial pH (x_1, A: p < 0.0066), initial HA concentration (x_2, B: p < 0.0001), and the interaction terms of AD: p = 0.0053 and BE: p = 0.0137, as well as the quadratic effect of E^2: p = 0.0060 were found to be more significant than the other independent factors, which was obvious from their corresponding values of Probability (p) > F. The results indicated that A, B, E, AD, BE, and E^2 to be significant model terms for the present EF system (Table 3).

Table 3. Results of statistical analysis employed on the quadratic model for HA removal.

Statistical indicator	Value	Statistical indicator	Value
Std. Dev.	2.72	R-squared (R^2)	0.8853
Mean	10.63	Adj. R-squared (R^2_{adj})	0.8532
C.V. %	25.61	Pred. R-squared (R^2_{pred})	0.7985
PRESS	325.46	Adeq. Precision (AP)	17.356

In Table 3, Std. Dev. refers the standard deviation or square root of the pure error (σ); Mean denotes the overall mean of response; C.V. indicates the coefficient of variation or standard deviation as a percentage of the mean; PRESS connotes the predicted residual sum of squares; R^2 shows the determination coefficient; R^2_{adj} expresses the adjusted determination coefficient; R^2_{pred} explains the predicted determination coefficient which is a measure of the predictive performance of the model; and

AP stands for the adequate precision, as a comparison of the range of the predicted values at the design points against the average prediction error.

Considering the results acquired from the ANOVA (Table 2), the percentage of contributions (PC) were computed for the first-order (*A*, *B*, *D*, *E*), the interaction (*AD*, *BE*), and the quadratic (E^2) terms according to the sum of squares (*SS*) of each individual components of the reduced quadratic model. The results showed that the initial HA concentration (x_2: *B*) yielded the highest contribution level (80.06%) among the other variables. This was tracked by the contributions of the initial pH (x_1 = *A*) and pulse time (x_5 = *E*) with PC values of 4.49% and 2.83%, respectively. The last part of the ANOVA was performed in the same manner for the computation of the total PC values (TPC) of the reduced quadratic models computing the first-order, the interaction, and the quadratic factors in the respective order as follows [22,23,26]:

$$TPC_i(\%) = \frac{\sum_{i=1}^{n} SS_i}{\sum_{i=1}^{n}\sum_{j=1}^{n} SS_i + SS_{ii} + SS_{ij}} \times 100 \quad (15)$$

$$TPC_{ij}(\%) = \frac{\sum_{i=1}^{n}\sum_{j=1}^{n} SS_{ij}}{\sum_{i=1}^{n}\sum_{j=1}^{n} SS_i + SS_{ii} + SS_{ij}} \times 100 \quad (16)$$

$$TPC_{ii}(\%) = \frac{\sum_{i=1}^{n} SS_{ii}}{\sum_{i=1}^{n}\sum_{j=1}^{n} SS_i + SS_{ii} + SS_{ij}} \times 100 \quad (17)$$

where TPC_i, TPC_{ii}, and TPC_{ij} denote the total percentage contributions (TPC) of the first-order, the interaction, and the quadratic terms, respectively. In the same manner, SS_i, SS_{ij}, and SS_{ii}, are the computed sums of squares for the first-order, the interaction, and the quadratic terms, respectively. A pictorial description of the PC of every distinct model variables is depicted in Figure 2. As demonstrated in Figure 2, the TPC of the first-order terms (TPC_i) revealed the highest level (TPC_i = 87.41%) when compared to those obtained from the others, and this was tracked by the TPC of the interaction terms (TPC_{ij} = 7.97%). On the contrary, the TPC of the interaction terms yielded the lowest magnitude of impact with a total contribution of TPC_{ij} = 7.51%, revealing that the interaction components did not have a considerable impact on modeling of the HA removal. In accordance with the above findings, the TPC values also indicated that the first-order independent factors (except the voltage, x_4: *D*) had a direct impact on the response component.

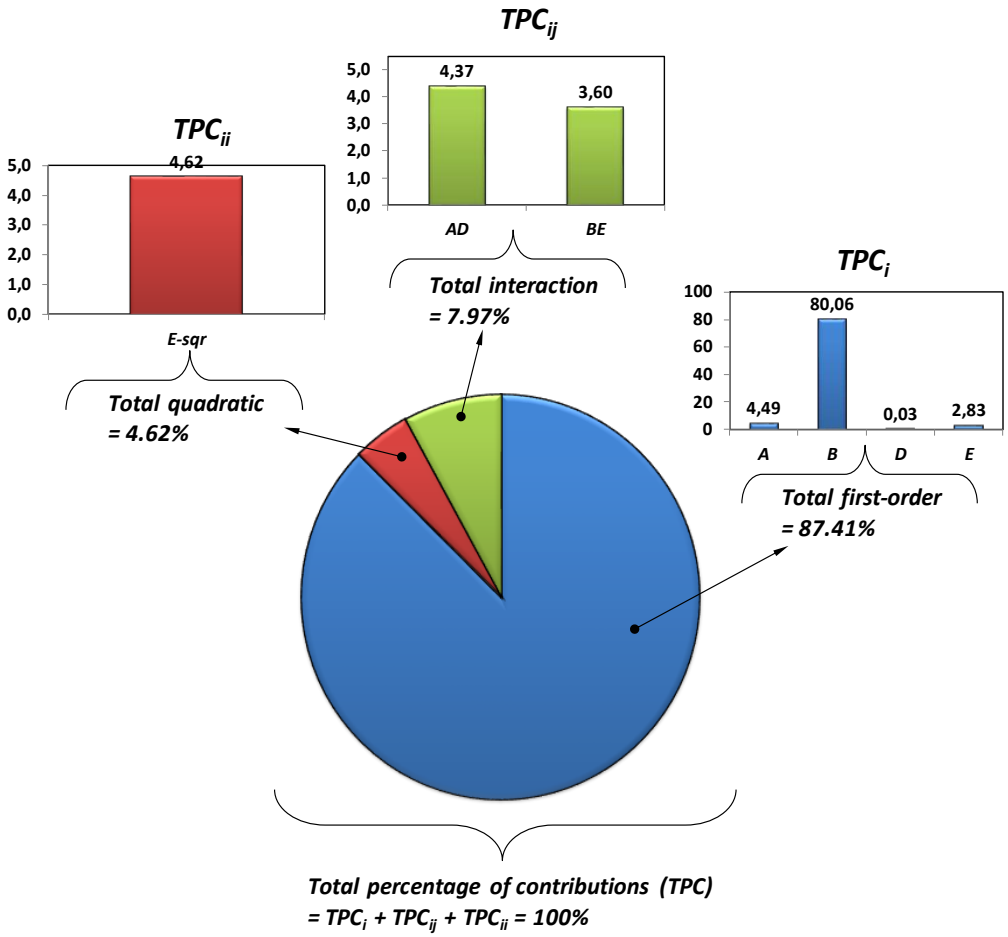

Figure 2. Pictorial description of the percentage contributions of the reduced quadratic model components.

The consequent form of the regression model consisting of the coded factors is described by the following second-order polynomial equation:

$$HA\ removal\ (mg) = 12.19 - 1.90A + 8.02B + 0.15D + 4.53E + 6.24AD - 1.80BE - 2.86E^2$$
$$subjected\ to\ -1 \le A - E \le 1 \quad (18)$$

Based on the actual factors, an empirical relationship was expressed between HA removal efficiency and the variables in the following second-order polynomial equation:

$$HA\ removal\ (mg) = 6.575 - 3.037(pH) + 0.512(HA\ Conc.) - 0.914(Volt.) + 0.158(Pul.\ time)$$
$$+0.143(pH \times Volt.) - 0.001(HA\ Conc. \times Pul.\ time) - 0.000353(Pul.\ time)^2 \quad (19)$$

In development of the surface response and contour plots of the second-order model, two variables were held at their center levels and the remaining components were altered within their experimental domain (Figure 3). In Figure 3a, the response surface and contour plot were created as a function of HA concentration and pulse time. In these graphs, the initial pH, electrical conductivity, voltage, and reaction time were kept constant at 6.50, 1750, 17.5, and 35, respectively. As can be seen in Figure 3a, the HA concentration and pulse time demonstrate a positive impact on the amount of HA removal. In other words, increases in the values of these variables significantly improve the performance of the system. In Figure 3b, the response surface and contour plot were established as a

function of initial pH and voltage, in which the HA concentration, electrical conductivity, pulse time, and reaction time were held constant at 30, 1750, 110, and 35, respectively. As can be seen from Figure 3b, the variables of pH and voltage variables have an opposite effect on the amount of HA removal, with the elevated values in these components noticeably reducing the performance of the system.

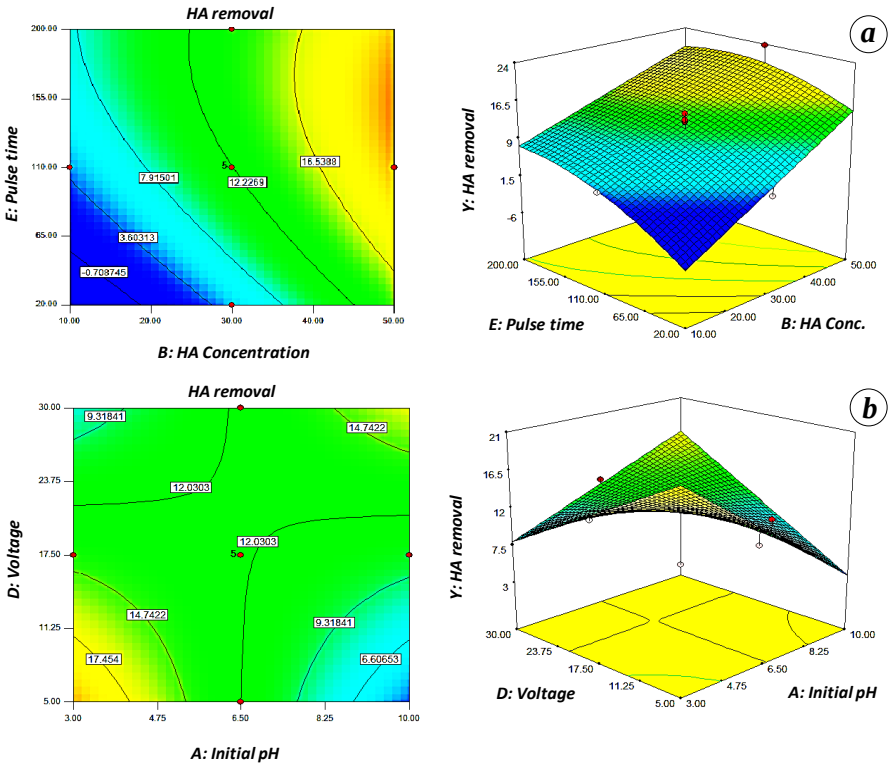

Figure 3. Surface response and contour plots illustrating the impact of (a) HA concentration and pulse time and (b) initial pH and applied voltage on HA removal (mg).

Consequently, the removal of HA was optimized through the use of Design-Expert 7 software. The optimization module in Design-Expert explores a combination of factor levels that concurrently fulfill the needs associated with each of the responses and factors. In line with the purpose of the optimization, one of the solutions offered by the software was selected by the authors. For the best forecast of HA removal efficiency, the optimum operating condition of the model components, with a desirability level of 0.871, was attained with an initial HA concentration 20 mg/L, initial pH 6, electrical conductivity 526 µS/cm, pulse time 200 min, voltage 5 V, and reaction time 10 min.

4. CONCLUSIONS

A six-factor (initial HA concentration, initial pH, electrical conductivity, pulse time, voltage, and reaction time) three-level central composite experimental design within the frame of RSM-based optimization was conducted as a powerful computational analysis approach to the modeling of a proposed pulse current EF process for the removal of HA from aqueous solutions. The observational

and model-based findings of the current analysis are outlined below, followed by some concluding remarks:

(1) An efficiency of 97.2 percent may be achieved in the removal of HA with the minimum electrical energy usage (1.02 kWh/kg HA removal) under the following operating conditions: initial HA concentration 50 mg/L, initial pH 3, electrical conductivity 500 μS/cm, pulse time 20 min, voltage 5 V, and reaction time 60 min.

(2) The RSM-based experimental design approach was successfully implemented for the modeling and optimization of HA removal. The results of the analysis revealed the optimum operating conditions of the variables associated with the EF process for the best prediction of HA removal efficiency with a desirability value of 0.871, to be initial HA concentration 20 mg/L, initial pH 6, electrical conductivity 526 μS/cm, pulse time 200 min, voltage 5 V, and reaction time 10 min.

(3) The suitability of the derived model was tested based on the several distinct statistical performance evaluators. The forecasted data obtained from the quadratic model equation closely resembled the experimental data. For the best-fit quadratic model, the R^2 value was determined to be 0.885, and the predicted R^2 of 0.7985 was in agreement with the adjusted R^2 of 0.8532. According to the results of the central composite design (CCD)-based analysis, HA concentration and pulse time had a favorable influence on the level of HA removal, while the initial pH and applied voltage had an opposite impact on the response variable.

(4) The statistical results revealed that the most influential variable in the second-order model was the initial HA concentration for the studied EF system ($p < 0.0001$, $F_{cal} = 156.25$, $TPC_i = 80.06\%$). The study findings also revealed that the TPC of the first-order terms yielded the highest magnitude of importance with a total contribution of 87.41 percent when compared with the respective TPC values of the quadratic and the interaction terms.

(5) Based on the experimental results obtained from this analysis, it is worthwhile to refer that the proposed EF process could be utilized as an efficacious and encouraging technology for the photocatalytic removal of humic substances from aqueous environments.

ACKNOWLEDGEMENTS

This manuscript has been prepared within the framework of a project that was approved by the Student Research Committee, and has been funded by the Kurdistan University of Medical Sciences (IR.MUK.REC.1394/78). It has been supported financially by the Turkish Academy of Sciences (TÜBA) as a part of Prof. Dr. Kaan Yetilmezsoy's "The Outstanding Young Scientist Award (TÜBA-GEBİP)" of the year 2018. The authors express their special thanks to the sponsors of the project.

References

1. A. Mahvi, A. Maleki, R. Rezaee and M. Safari, *Iranian Journal of Environmental Health, Science and Engineering*, 6 (2009) 233.
2. G. Hasani, H. Daraei, B. Shahmoradi, F. Gharibi, A. Maleki, K. Yetilmezsoy and G. McKay, *Process Safety and Environmental Protection*, 117 (2018) 111.
3. X-F. Zhou, J-P. Liang, Z-L. Zhao, H. Yuan, J-J. Qiao, Q-N. Xu, H-L. Wang, W-C., Wang and D-Z. Yang, *Journal of Hazardous Materials*, 403 (2020) 123626.

4. S.M. Pormazar, M.H. Ehrampoush, M.T. Ghaneian, M. Khoobi, P. Talebi and A. Dalvand, *Korean Journal of Chemical Engineering*, 37 (2020) 93.
5. A., Barhoumi, S. Ncib, A. Chibani, K. Brahmi, W. Bouguerra and E. Elaloui, *Industrial Crops and Products*, 140 (2019) 111715
6. M.S. Algamdi, I.H. Alsohaimi, J. Lawler, H.M. Ali, A.M. Aldawsari and H.M. Hassan, *Separation and Purification Technology*, 223 (2019) 17.
7. A. Andersson, E. Lavonen, M. Harir, M. Gonsior, N. Hertkorn, P. Schmitt-Kopplin, H. Kylin, and D. Bastviken, *Environmental Science: Water Research & Technology*, 6 (2020) 779-794.
8. Y. Wang, Q. Wang, B.-Y. Gao, Q. Yue and Y. Zhao, *Chemical Engineering Journal*, 193 (2012) 59.
9. M.S. Rauthula and V.C. Srivastava, *Chemical Engineering Journal*, 168 (2011) 35.
10. A. El-Ghenymy, M. Alsheyab, A. Khodary, I. Sirés and A. Abdel-Wahab, *Chemosphere*, 246 (2020) 125674.
11. M.S. Algamdi, I.H. Alsohaimi, J. Lawler, H.M. Ali, A.M. Aldawsari and H.M. Hassan, *Separation and Purification Technology*, 223 (2019) 17.
12. M.N. Moura, M.J. Martín and F.J. Burguillo, *Journal of Hazardous Materials,* 149 (2007) 42.
13. P. Finkbeiner, G. Moore, R. Pereira, B. Jefferson and P. Jarvis, *Chemosphere*, 238 (2020) 124633.
14. D. Ghernaout and N. Elboughdiri, *Open Access Library Journal*, 7 (2020) e6139.
15. V. Austen, C. Suyitno, T.Y.P.R. Gah, P. Sugiart, S.P. Santoso, F.E. Soetaredjo, K. Foe, A.E. Angkawidjaja, Y-H. Ju, S. Ismadji, *Journal of the Indonesian Chemical Society*, 3 (2020) 1.
16. S. Vasudevan and M.A. Oturan, *Environmental Chemistry Letters*, 12 (2014) 97.
17. I. Sirés, E. Brillas, M.A. Oturan, M.A. Rodrigo and M. Panizza, *Environmental Science and Pollution Research*, 21 (2014) 8336.
18. S. Garcia-Segura, F. Centellas, C. Arias, J.A. Garrido, R.M. Rodríguez, P.L. Cabot and E. Brillas, *Electrochimica Acta*, 58 (2011) 303.
19. S.R. Patel and S.P. Parikh, *Arabian Journal of Chemistry*, 13 (2020) 7032.
20. M. Hadi, G. McKay, M.R. Samarghandi, A. Maleki and M. Solaimany Aminabad, *Desalination and Water Treatment*, 49 (2012) 81.
21. R. Rezaee, A. Maleki, A. Jafari, S. Mazloomi, Y. Zandsalimi and A.H. Mahvi, *Journal of Environmental Health Science and Engineering*, 12 (2014) 67.
22. M. Foroughi, S. Chavoshi, M. Bagheri, K. Yetilmezsoy and M.T. Samadi, *Journal of Material Cycles and Waste Management*, 20 (2018) 1999.
23. K. Yetilmezsoy, S. Demirel and R.J. Vanderbei, *Journal of Hazardous Materials*, 171 (2009) 551.
24. M. Sepehr Noori, K. Yetilmezsoy, S. Marofi, M. Zarrabi, H.R. Ghaffari, M. Fingas and M. Foroughi, *Journal of the Taiwan Institute of Chemical Engineers*, 45 (2014) 2786.
25. A.T. Nair and M.M. Ahammed, *Journal of Cleaner Production*, 96 (2015) 272.
26. H. Meng, X. Hu and A. Neville, *Wear*, 263 (2007) 355.